J|A|C|S
COMMUNICATIONS

Amphiphilic Molecular Design as a Rational Strategy for Tailoring Bicontinuous Electron Donor and Acceptor Arrays: Photoconductive Liquid Crystalline Oligothiophene−C_{60} Dyads

Wei-Shi Li,*,† Yohei Yamamoto,† Takanori Fukushima,*,†,‡ Akinori Saeki,§ Shu Seki,§ Seiichi Tagawa,§ Hiroyasu Masunaga,# Sono Sasaki,# Masaki Takata,#,∥ and Takuzo Aida*,†,‡

ERATO-SORST Nanospace Project, Japan Science and Technology Agency (JST), National Museum of Emerging Science and Innovation, 2-41 Aomi, Koto-ku, Tokyo 135-0064, Japan, Department of Chemistry and Biotechnology, School of Engineering and Center for NanoBio Integration, The University of Tokyo, 7-3-1 Hongo, Bunkyo-ku, Tokyo 113-8656, Japan, Institute of Scientific and Industrial Research (ISIR), Osaka University, 8-1, Mihogaoka, Ibaraki, Osaka 567-0047, Japan, Japan Synchrotron Radiation Research Institute (JASRI), 1-1-1 Kouto, Sayo-cho, Sayo-gun, Hyogo 679-5198, Japan, and RIKEN SPring-8 Center, 1-1-1 Kouto, Sayo-cho, Sayo-gun, Hyogo 679-5148, Japan

Received April 15, 2008; E-mail: li@nanospace.miraikan.jst.go.jp; fukushima@nanospace.miraikan.jst.go.jp; aida@macro.t.u-tokyo.ac.jp

Tailoring bicontinuous electron donor (D) and acceptor (A) arrays in solution-processable materials is an essential step for the realization of thin-film organic optoelectronics.[1] Casting of a D/A mixture may give rise to photoconductive bulk materials.[2] However, without proper choice of the components, many defects are usually formed, leading to trapping and rapid annihilation of charge carriers. In view of photovoltaics, the presence of bicontinuous D and A arrays is essential, but cast films from D/A mixtures likely contain their charge-transfer complexes. So far, nanofibers and tubes with bicontinuous D and A arrays have been obtained by self-assembly of covalently linked D−A dyads.[3,4] Nevertheless, solution-processable bulk materials with a D/A heterojunction[5] might be more realistic for device applications. Here we report a photoconductive liquid crystal (LC) with bicontinuous arrays of densely packed D and A components, tailored from amphiphilic oligothiophene−C_{60} dyad $\mathbf{1}_{\mathrm{Amphi}}$ (Chart 1).[6] Together with contrasting results for a nonamphiphilic reference ($\mathbf{1}_{\mathrm{Lipo}}$), we highlight a crucial role of the amphiphilic design both in structuring and in photoconductivity.

The molecular structures of $\mathbf{1}_{\mathrm{Amphi}}$ and $\mathbf{1}_{\mathrm{Lipo}}$ are identical to each other except for the terminal wedges. $\mathbf{1}_{\mathrm{Amphi}}$ bears a hydrophilic wedge with triethylene glycol chains and, on the other side, a hydrophobic wedge with paraffinic chains. In contrast, $\mathbf{1}_{\mathrm{Lipo}}$ possesses only the paraffinic wedges. We also prepared compounds **2** and **3**, which are equivalent to the donor and acceptor components of $\mathbf{1}_{\mathrm{Amphi}}$, respectively. They are all soluble in CH_2Cl_2, where the absorption spectral profiles (Figure S3) and redox properties (Figure S4) of $\mathbf{1}_{\mathrm{Amphi}}$ and $\mathbf{1}_{\mathrm{Lipo}}$ were essentially identical to one another.[6]

Dyad $\mathbf{1}_{\mathrm{Amphi}}$ formed a LC smectic A mesophase over a wide temperature range from 136.1 to 18.3 °C (Figure S5).[6] Polarized optical microscopy (POM) of LC-$\mathbf{1}_{\mathrm{Amphi}}$ displayed a typical focal-conic texture (Figure 1a). Synchrotron radiation small-angle X-ray scattering (SAXS) analysis showed sharp peaks with *d* spacings of 10.6, 5.3, 3.5, and 2.6 nm (Figure 1c), which can be indexed as (100), (200), (300), and (400) reflections of a lamellar structure with a layer width of 10.6 nm. On the basis of a CPK model of $\mathbf{1}_{\mathrm{Amphi}}$, the observed layer width is almost twice as large as the distance from the paraffinic end to the fullerene unit (~5.5 nm; Figure 2, I). Thus, each repeating layer consists of laterally coupled tail-to-tail pairs of $\mathbf{1}_{\mathrm{Amphi}}$, and such layers are connected at the fullerene-appended hydrophilic head part of $\mathbf{1}_{\mathrm{Amphi}}$ to form a 2D lamellar structure. In this configuration, the hydrophilic and paraffinic wedges are separated by 5.3 nm.

Chart 1. Structures of $\mathbf{1}_{\mathrm{Amphi}}$, $\mathbf{1}_{\mathrm{Lipo}}$, and References **2** and **3**

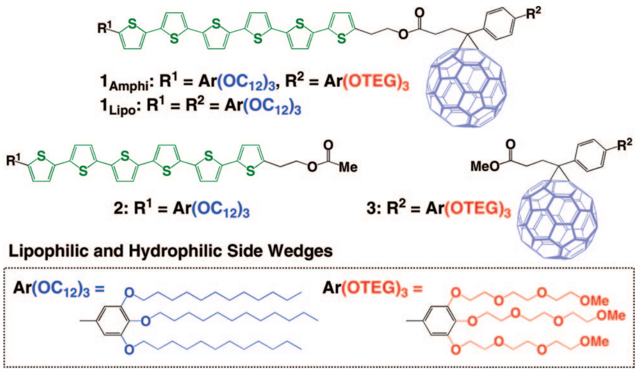

Similar to $\mathbf{1}_{\mathrm{Amphi}}$, nonamphiphilic $\mathbf{1}_{\mathrm{Lipo}}$ formed a smectic A LC mesophase in a temperature range from 111.4 to 12.5 °C, as

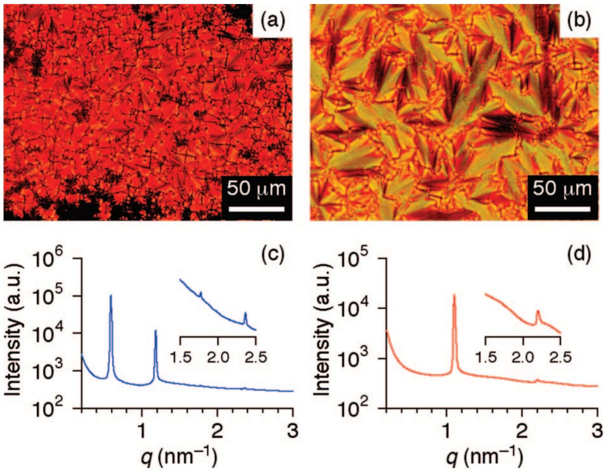

Figure 1. POMs at 33 °C and SAXS patterns at 30 °C (inset: magnified at $q = 1.5{-}2.5\ nm^{-1}$) of (a,c) LC-$\mathbf{1}_{\mathrm{Amphi}}$ and (b,d) LC-$\mathbf{1}_{\mathrm{Lipo}}$.

[†] ERATO-SORST Nanospace Project, JST.
[‡] The University of Tokyo.
[§] Osaka University.
[#] JASRI.
[∥] RIKEN.

10.1021/ja802757w CCC: $40.75

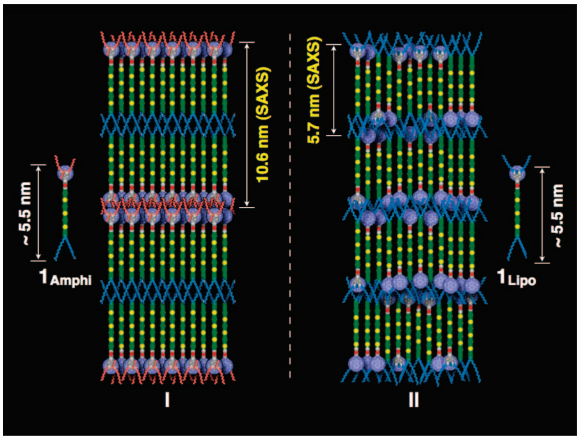

Figure 2. Schematic representations of molecular orientations in LC-$\mathbf{1}_{\mathbf{Amphi}}$ (I) and LC-$\mathbf{1}_{\mathbf{Lipo}}$ (II) with a smectic A mesophase.

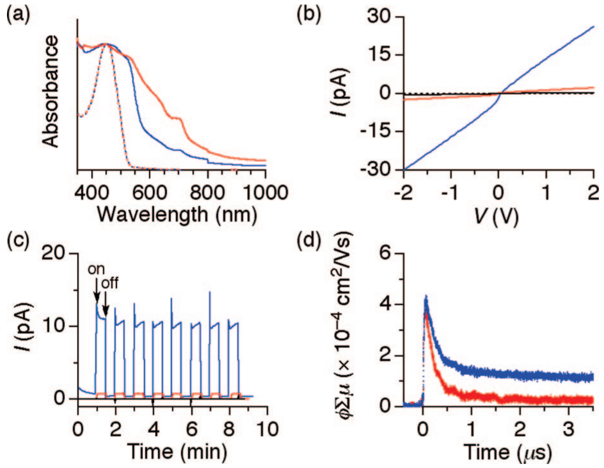

Figure 3. (a) Absorption spectra at 25 °C of $\mathbf{1}_{\mathbf{Amphi}}$ (blue) and $\mathbf{1}_{\mathbf{Lipo}}$ (red) in the LC state (solid curves) and in CH_2Cl_2 (broken curves), normalized at 450 nm. Photoconducting properties at 25 °C of LC-$\mathbf{1}_{\mathbf{Amphi}}$ (blue), LC-$\mathbf{1}_{\mathbf{Lipo}}$ (red), and a 1:1 mixture of **2** and **3** (black); (b) $I-V$ profiles without (broken curves) and with photoirradiation (solid curves) and (c) changes in photogenerated electric current under an applied voltage of +1 V. (d) FP-TRMC profiles (λ_{ex} = 355 nm) of LC-$\mathbf{1}_{\mathbf{Amphi}}$ (blue) and LC-$\mathbf{1}_{\mathbf{Lipo}}$ (red).

observed by DSC and POM profiles (Figures 1b and S5).[6] SAXS pattern (Figure 1d) displayed intense and weak diffractions with d spacings of 5.7 and 2.9 nm, respectively, which were indexed as (100) and (200) reflections of a lamellar structure with a layer width of 5.7 nm (Figure 2, II). The observed width is close to the molecular length of $\mathbf{1}_{\mathbf{Lipo}}$. Considering that both ends of $\mathbf{1}_{\mathbf{Lipo}}$ are paraffinic, the head/tail orientation of $\mathbf{1}_{\mathbf{Lipo}}$ in the lamellar structure is most likely nonuniform (Figure 2, II). In relation to these structural aspects, the absorption spectrum of LC-$\mathbf{1}_{\mathbf{Lipo}}$ was different from that of LC-$\mathbf{1}_{\mathbf{Amphi}}$, while both were obviously broader than those in CH_2Cl_2 (Figure 3a). In particular, a broad band observed for LC-$\mathbf{1}_{\mathbf{Lipo}}$ at 600−800 nm suggests a charge-transfer interaction between the oligothiophene and fullerene units, which can occur unless $\mathbf{1}_{\mathbf{Lipo}}$ adopts a uniform head/tail orientation.

As shown in Figure 3b,c, LC-$\mathbf{1}_{\mathbf{Amphi}}$ (blue) exhibited a distinct photoconductive character. At an applied voltage of, for example, +2 V, the current at 25 °C increased abruptly from 0.09 to 26 pA (on/off ratio = 290) upon irradiation and quickly retrieved the original value when the light was turned off. In contrast, a 1:1 mixture of **2** and **3** formed neither regular structures nor photoconductivity (black). Noteworthy, LC-$\mathbf{1}_{\mathbf{Lipo}}$ (red) was much less conductive than LC-$\mathbf{1}_{\mathbf{Amphi}}$, where the photocurrent was only 1/10 that of $\mathbf{1}_{\mathbf{Amphi}}$ observed under identical conditions. This result is interesting since the electron transfer efficiencies in LC-$\mathbf{1}_{\mathbf{Amphi}}$ and LC-$\mathbf{1}_{\mathbf{Lipo}}$, judging from their fluorescence quenching profiles (Figure S6),[6] are considered equally high. Having these features in mind, we conducted flash photolysis time-resolved microwave conductivity (FR-TRMC) measurements, which are informative of the behaviors of mobile charge carriers in a short distance (~10 nm). With a 355 nm laser pulse at 25 °C (Figure 3d), the maximum conductivity ($\phi\Sigma\mu_{\max}$ in cm^2/V·s) of LC-$\mathbf{1}_{\mathbf{Amphi}}$ (4.1×10^{-4}) was markedly greater than that of the **2**/**3** mixture (1.2×10^{-4}) but almost comparable to that of LC-$\mathbf{1}_{\mathbf{Lipo}}$ (3.7×10^{-4}). However, the charge carrier, generated in LC-$\mathbf{1}_{\mathbf{Lipo}}$, was shorter-lived than that in LC-$\mathbf{1}_{\mathbf{Amphi}}$, suggesting the presence of a larger number of trapping sites in LC-$\mathbf{1}_{\mathbf{Lipo}}$. This is in accord with the aforementioned low structural integrity of LC-$\mathbf{1}_{\mathbf{Lipo}}$ (Figure 2, II) and its poor photoconducting nature in a macroscopic scale (Figure 3b).

In summary, we have demonstrated that amphiphilic molecular design[7] can be a rational strategy for the spontaneous formation of bicontinuous donor and acceptor arrays in liquid crystalline materials. Site-specific modification of donor−acceptor dyads with hydrophilic and paraffinic wedges not only prohibits donor−acceptor interactions leading to the trapping of charge carriers but also ensures a long-range conducting pathway in the materials. As liquid crystals are solution-processable and self-healable, our design strategy may contribute to the development of high-performance organic optoelectronics.

Acknowledgment. The synchrotron radiation experiments were carried out on the BL40B2 of SPring-8 under the Priority Nanotechnology Support Program administrated by JASRI (Proposal No. 2008A1650).

Supporting Information Available: Details of synthesis and characterization of $\mathbf{1}_{\mathbf{Amphi}}$, $\mathbf{1}_{\mathbf{Lipo}}$, **2**, and **3**, and supporting Figures S1−S6. This material is available free of charge via the Internet at http://pubs.acs.org.

References

(1) (a) Segura, J. L.; Martín, N.; Guldi, D. M. *Chem. Soc. Rev.* **2005**, *34*, 31–47. (b) Günes, S.; Neugebauer, H.; Sariciftci, N. S. *Chem. Rev.* **2007**, *107*, 1324–1338. (c) Thompson, B. C.; Fréchet, J. M. J. *Angew. Chem., Int. Ed.* **2008**, *47*, 58–77.
(2) (a) Percec, V.; Glodde, M.; Bera, T. K.; Miura, Y.; Shiyanovskaya, I.; Singer, K. D.; Balagurusamy, V. S. K.; Heiney, P. A.; Schnell, I.; Rapp, A.; Spiess, H.-W.; Hudsonk, S. D.; Duank, H. *Nature* **2002**, *419*, 384–387. (b) Schmidt-Mende, L.; Fechtenkötter, A.; Müllen, K.; Moons, E.; Friend, R. H.; MacKenzie, J. D. *Science* **2006**, *293*, 1119–1122. (c) Liscio, A.; De Luca, G.; Nolde, F.; Palermo, V.; Müllen, K.; Samorì, P. *J. Am. Chem. Soc.* **2008**, *130*, 780–781.
(3) (a) Yamamoto, Y.; Fukushima, T.; Suna, Y.; Ishii, N.; Saeki, A.; Seki, S.; Tagawa, S.; Taniguchi, M.; Kawai, T.; Aida, T. *Science* **2006**, *314*, 1761–1764. (b) Yamamoto, Y.; Fukushima, T.; Saeki, A.; Seki, S.; Tagawa, S.; Ishii, N.; Aida, T. *J. Am. Chem. Soc.* **2007**, *129*, 9276–9277.
(4) (a) Würthner, F.; Chen, Z.; Hoeben, F; J, M.; Osswald, P.; You, C.-C.; Jonkheijm, P.; Herrikhuyzen, J. v.; Schenning, A. P. H. J.; van der Schoot, P. P. A. M.; Meijer, E. W.; Beckers, E. H. A.; Meskers, S. C. J.; Janssen, R. A. J. *J. Am. Chem. Soc.* **2004**, *126*, 10611–10618. (b) Röger, C.; Müller, M. G.; Lysetska, M.; Miloslavina, Y.; Holzwarth, A. R.; Würthner, F. *J. Am. Chem. Soc.* **2006**, *128*, 6542–6543.
(5) (a) Samorì, P.; Yin, X.; Tchebotareva, N.; Wang, Z.; Pakula, T.; Jackel, F.; Watson, M. D.; Venturini, A.; Müllen, K.; Rabe, J. P. *J. Am. Chem. Soc.* **2004**, *126*, 3567–3575. (b) Peeters, E.; van Hal, P. A.; Meskers, S. C. J.; Janssen, R. A. J.; Meijer, E. W. *Chem.—Eur. J.* **2002**, *8*, 4470–4474.
(6) See Supporting Information.
(7) For review, see: Tschierske, C. *J. Mater. Chem.* **2001**, *11*, 2647–2671.

JA802757W